

# Urban Area End Logistics Drones Distribution Route Planning

Fang Tan<sup>1, \*</sup>

<sup>1</sup> School of Modern Post, Chongqing University of Posts and Telecommunications, Chongqing 400065, China

\* Corresponding author: Fang Tan (Email: 1300835669@qq.com)

**Abstract:** With the development of logistics technology, the application of drones in the last mile of logistics distribution has also become a hot topic. Due to the complexity and particularity of the flight environment in urban areas, UAVs need to comprehensively consider safety performance and flight energy consumption when conducting terminal logistics distribution. Based on this, this paper constructs a mathematical model with the goal of shortening flight paths, reducing energy consumption, and improving flight safety, and completes environmental modeling using grid method and genetic algorithm to solve the model. At the same time, the battery energy consumption of the UAV is calculated using the energy consumption segmentation mode. The experimental results of a numerical example verify the effectiveness of the model and algorithm, and also prove that considering segmented energy consumption can more accurately calculate the battery energy consumption of unmanned aerial vehicles.

**Keywords:** UAV, Path optimization, Genetic algorithm.

## 1. Introduction

The development of e-commerce and the progress of technology have promoted the change of logistics distribution. unmanned aerial vehicle (UAV), as a new distribution tool, has attracted wide attention. Since 2013, when e-commerce giant Amazon announced its drone delivery plan, domestic and foreign logistics related enterprises have also actively participated in the research and development of the practical application of drones, which has also promoted the improvement and development of UAV technology to a certain extent. However, due to the constraints of UAV flight distance, load and other factors [1] and the complexity of urban flight environment [2], how to plan the terminal distribution path more reasonably on the premise of ensuring the flight safety of UAV has also become a problem that needs to be studied and discussed.

At present, the literature on UAV routing optimization mainly focuses on the combined transport mode, routing optimization algorithm and safety obstacle avoidance. Peng and Liu [3,4] studied and established the mathematical model of vehicle and UAV cooperative delivery service, and verified that the "UAV-vehicle" joint distribution and transportation mode can effectively improve the efficiency of logistics distribution. In addition to improving the difference algorithm. Ren [5] also proposes a calculation method of energy consumption segmentation model, which can more accurately calculate the battery energy consumption of UAV. Huang and Zhang [6,7] improved the defects of genetic algorithm and RRT algorithm respectively, and proposed an improved UAV path planning algorithm. Zhang [8] established an objective function based on the minimum flight time, battery energy consumption, and risk of drones, and studied the drone navigation planning between two freight warehouses in urban areas. Yang [9] studied the path planning scheme of mobile robot considering path obstacle avoidance. Z. Kewang [10] proposes an obstacle avoidance path planning method for multiple UAVs based on model predictive control for obstacle avoidance control.

To sum up, the existing literature on the urban end logistics UAV route planning is generally less, and the content is mostly focused on the UAV safety obstacle avoidance or path planning algorithm improvement, and the literature on the comprehensive consideration of safety, energy consumption and multi-demand point distribution is less. In view of this, this paper mainly studies the route optimization of urban end-logistics UAV under multi-demand tasks. Its objective function is to consider the minimum comprehensive cost under safety obstacle avoidance, battery energy consumption and path length, and solve the problem through genetic algorithm. At the same time, energy consumption segmentation is used to calculate the battery energy consumption of UAV during flight, so as to make it more suitable for the practical situation.

## 2. Path Planning Model

### 2.1. Problem description and model assumptions

#### 2.1.1. Problem Description

The UAV path planning studied in this paper is applicable to the logistics distribution service from single distribution center to multiple customer points. In order to verify the effectiveness of the proposed algorithm in path planning, the terrain elevation, building height and contour data of 1000m×1000m of urban area were obtained by using Baidu Map, and this area was taken as the application scene of this path planning.

#### 2.1.2. Model assumptions

(1) the distribution center and demand point coordinates are known, the  $i, j$  for demand point (path point) number ( $i, j \in [0, n]$ ),  $C_i$  collection for demand point,  $C_0$  table distribution center,  $u$  for unmanned aerial vehicle (uav) code; (2) The maximum load of the UAV is  $Q_{max}$ , which can carry multiple packages at a time within the load-bearing range; (3) The maximum flight distance of UAV is  $D_{max}$ , which is determined by flight power and battery capacity; (4) The

drone's battery is fully charged at the beginning of delivery, and the maximum battery energy is  $E_{max}$ ; (5) Drones do not accept midway assignments during the delivery process. (6) Return to the distribution center after completing the distribution task; (7) The delivery order of demand points is known.

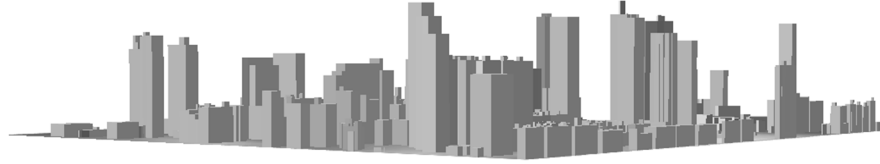


Figure 1. 3D flight environment modeling diagram

(2) Convert 3D to 2D environment modeling. As the flight height limit of low-altitude logistics UAV is generally between 70 and 120 meters, For obstacles below the minimum flight altitude, drones can directly cross them by leaping, while for obstacles between flight altitudes, drones need to detour and avoid them. In order to simplify the environmental model, environmental data between 70 and 120 meters are retained after ArcGis screening, and obstacles in this part of the environment are represented on a two-dimensional plane (output). Then the two-dimensional grid is used for approximate unit decomposition of terrain. If there are terrain and obstacles, the value is 1, otherwise 0. In this paper, grid granularity (1) refers to the literature [8] and considers the width of buildings in the flight area. Set  $l=10m$ . The obstacle distribution in two-dimensional grid environment is shown in the figure below.

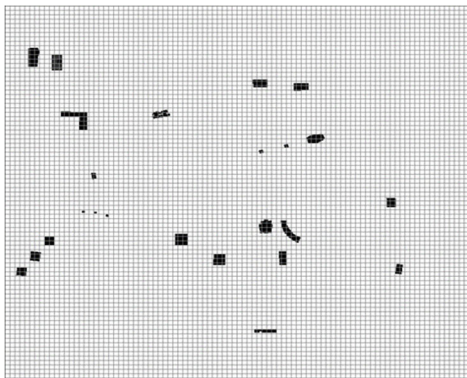


Figure 2. Schematic diagram of 2D grid environment modeling

## 2.3. Drone Energy Consumption Model

### 2.3.1. Objective function

(1) Calculation of flight distance

$d_{ij}$  represents the flight distance from path point  $i$  to  $j$ , and  $(x_i, y_i)$  is the coordinate of point  $i$ , using Euclidean distance calculation. The sum of each flight distance is the total flight distance of UAV, denoted by  $D$ :

$$D = \sum_{i=0}^n \sum_{j=0}^n \sqrt{(x_i - x_j)^2 + (y_i - y_j)^2} \quad (1)$$

(2) Flight risk calculation

In this paper, static objects such as urban buildings and terrain were mainly considered for UAV obstacle avoidance.

## 2.2. Grid environment modeling

(1) First, Baidu Map was used to obtain the terrain elevation, building height and contour data of the UAV flight area, and then ArcScene in ArcGis software was used to complete the three-dimensional environment modeling.

$N_r$  was set to represent the number of obstacle grids near waypoint  $i$  to  $j$ , and  $N_t$  was set to represent the total number of all grids around waypoint  $i$  to  $j$ . The formula for calculating the risk degree  $r_{ij}$  is:

$$r_{ij} = \frac{N_r}{N_t} \quad (2)$$

Let the total cost of flight risk be represented by  $R$ , and risk penalty factor be  $k$ :

$$R = \sum_{i=0}^n \sum_{j=0}^n k r_{ij} \quad (3)$$

(3) Calculation of flight energy consumption:

The cargo weight is represented by  $q_{ij}$ , the dead weight of UAV is  $m$ , the flight speed is  $v_{ij}$ , the flight time is  $t_{ij}$ , the power transmission efficiency of propeller is  $\mu$ , the lift-drag ratio is  $\gamma$ , the energy consumption of electronic components is  $p$ , and the battery power is  $e_{ij}$ . Uav battery power calculation reference [11]:

$$e_{ij} = \frac{(q_{ij} + m)v_{ij}}{370\mu\gamma} + p \quad (4)$$

Uav flight battery energy consumption is expressed by  $E_{ij}$ :

$$E_{ij} = e_{ij}t_{ij} \quad (5)$$

Let the total energy consumption cost of flight battery be represented by  $E$ :

$$E = \sum_{i=0}^n \sum_{j=0}^n x_{iju} e_{ij} t_{ij} = \sum_{i=0}^n \sum_{j=0}^n x_{iju} e_{ij} \frac{d_{ij}}{v_{ij}} \quad (6)$$

Due to the fact that the energy consumption of flight batteries is directly proportional to the flight distance, and the path length  $d_{ij}$  is included in the calculation formula  $E$  of the total battery energy consumption cost, no more repeated calculations in the overall objective function. To sum up, the formula of total objective function (comprehensive cost) is as follows:

$$\min \varphi = \omega_1 E + \omega_2 R \quad (7)$$

The objective function represents the minimum flight path, energy consumption and risk of logistics UAV on the premise of meeting the task requirements.  $\omega_1$  is the weight coefficient of the total energy consumption cost of the battery,  $\omega_2$  is the weight coefficient of the risk cost, which satisfies:

$$\omega_1 + \omega_2 = 1 \quad (8)$$

### 2.3.2. Constraints

$$x_{iju} = [0, 1] \quad (i, j \in C_i, i \neq j) \quad (9)$$

$$\sum_{i=0}^n x_{iju} = 1 \quad (i \in C_i) \quad (10)$$

$$\sum_{j=0}^n x_{iju} = 1 \quad (j \in C_i) \quad (11)$$

$$\sum_{i=0}^n x_{iju} = \sum_{i=0}^n x_{jiu} \quad (i, j \in C_i, i \neq j) \quad (12)$$

$$\sum_{j=1}^n x_{0ju} = \sum_{j=1}^n x_{j0u} \quad (j \in C_i) \quad (13)$$

$$\sum_{i=0}^n \sum_{j=0}^n x_{iju} e_{ij} \frac{d_{ij}}{v_{ij}} \leq E_{\max} \quad (i, j \in C_i, i \neq j) \quad (14)$$

$$\sum_{i=0}^n \sum_{j=0}^n x_{iju} q_{ij} \leq Q_{\max} \quad (i, j \in C_i, i \neq j) \quad (15)$$

Where, Formula (9) is a decision scalar, indicating that the unmanned aerial vehicle  $u$  completes the allocation tasks from demand points  $i$  to  $j$ , which is 1. Otherwise, it is 0. Equations (10) and (11) indicate that all tasks need to be completed. Equations (12) and (13) eliminate subpaths. Formula (14) indicates that the battery energy consumed by the range is less than the maximum energy. Formula (15) indicates that the total demand of UAV service is less than the maximum load.

## 3. Algorithm Flow

As the path planning problem solved in this paper has many constraints, the genetic algorithm of intelligent optimization algorithm is adopted to solve the problem and search for the global optimal from the population. The specific process of the algorithm is as follows:

### 3.1. Map Construction

(1) Construct obstacle grid map. For two-dimensional grid maps, assign a value of 1 to areas with obstacles and 0 to areas that can fly freely.

(2) Map coding. In this paper, decimal coding is adopted to encode from index 0 of the list in the upper left corner to the last grid in the lower right corner. The grid coordinates can be represented by  $(x_i, y_i)$ , the first grid coordinate in the upper left corner is  $(0,0)$ , the map code is 0,  $x_i$  increases from left to right,  $y_i$  increases from top to bottom.

### 3.2. Population initialization

One path generated by the algorithm in this paper is an individual. Set the population size  $Z$ , then input the starting point and end point coordinates, and select a free grid from each row between the starting point and the end point to form the initial path. In order to speed up path search and produce better individuals, free grid search is carried out from eight directions: top, bottom, left, right, top left, bottom left and bottom right.

The path generated by population initialization may be continuous or discontinuous. Therefore, it is necessary to determine whether all adjacent grids in the path are continuous. The judging formula is as follows:

$$M = \text{Max}\{|x_i - x_{i+1}|, |y_i - y_{i-1}|\} \quad (16)$$

If  $M=1$ , then the path is continuous, otherwise it is discontinuous. For two discontinuous grids, it is necessary to calculate the midpoint grid  $(X_m, Y_m)$  between the two grids and perform continuity processing. The calculation formula is as follows:

$$X_m = \text{int}\left(\frac{x_i + x_{i+1}}{2}\right) \quad (17)$$

$$Y_m = \text{int}\left(\frac{y_i + y_{i+1}}{2}\right) \quad (18)$$

If  $(X_m, Y_m)$  is a free grid, it is inserted into the discontinuous grid. If  $(X_m, Y_m)$  is the obstacle grid, we need to re-determine and select the nearby free grid insertion that is not in the path. If no grid satisfies the condition after traversing the eight directions, the path is eliminated; Repeat the appeal procedure until the entire path is continuous or no continuous grid removal path can be found. The example of individual genes generated after path continuous operation is shown in Figure 3 below.

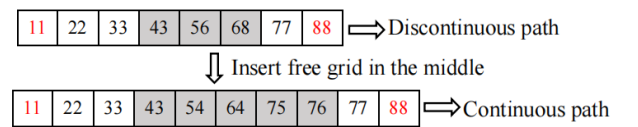


Figure 3. Examples of individual genes

### 3.3. Calculate individual fitness value

This algorithm sets the fitness value of the  $x$  individual as  $f_x = 1/(\omega_1 E + \omega_2 R)$ . The selected fitness function mainly includes the calculation of path length, flight energy consumption and risk cost.

### 3.4. Selection Operations

In this paper, the method of binary tournament is adopted to select the operation, and the method is as follows:

(1) First, determine the number of individuals selected each time as 2.

(2) Secondly, individuals in the population are randomly selected with the same probability, and the number of individuals selected is 2. The selection criteria are arranged according to the fitness values of the individuals, and the individuals with the best fitness values are retained and passed on to the next generation.

(3) Finally, the operation of step (2) is repeated until the number of individuals in the new population reaches the previous number.

### 3.5. Cross operation

Due to the varying lengths of individuals, for ease of operation, two adjacent individuals are selected to cross at the same encoding point except for the starting and ending points. At the same time, this article adopts a combination of single and double points for selection operations. The specific method is to form a group of all individuals retained after the selection operation in pairs in order (if the total number of individuals is odd, the last and first individuals will form a group). Set the crossover probability  $p_c$  and randomly generate  $r$  ( $r \in [0,1]$ ). If  $r < p_c$ , the crossover operation is performed. For paths that require crossover operations, first identify the number of identical points  $N$  in both paths, except for the start and end points. If  $N \geq 2$ , randomly select one of the single or double point intersections, and then randomly select the intersection point position from the same code for crossover; If  $N=1$ , use single point crossing; If  $N=0$ , directly reserve the path to enter the next generation.

### 3.6. Mutation Operation

The mutation operation method is: set the mutation probability  $p_m$ , and then randomly generate  $r$  ( $r \in [0,1]$ ). If  $r < p_m$ , then the mutation operation is performed. For the path that needs to undergo mutation operation, randomly select two grids in the path (except the starting point and the ending point) to delete all the waypoints between them, and then take these two points as the starting and ending points to insert the path point, so that the whole path is continuous. If the selected two grids cannot generate a continuous path after the operation, the two grids are selected again for execution until the mutation operation is complete.

### 3.7. Update Population

After performing the above operations, a population update is required. If the number of iterations is not reached or the optimal path is not generated at this time, the previous steps need to be repeated. On the contrary, the individual with the largest fitness value in the population is taken as the output of the optimal solution.

### 3.8. Path Smoothing

Grid based path planning may result in zigzag paths. Therefore, after the path planning is completed, the Freudian algorithm is used for path smoothing, which removes collinear points and excess turning points to make the drone's flight path smoother.

## 4. Path Planning Simulation Experiment

### 4.1. Experimental Data Selection and Parameter Settings

The experimental map in this article is a real map within a randomly selected range of 1000X1000m in the urban area. Firstly, ArcGis and Python are used to process the elevation and contour of buildings and complete grid environment modeling. Secondly, randomly select 5 free grids from the grid environment map to complete the construction of distribution centers and demand points. The distribution center point number is 0, and the demand point number is 1,2,3,4. Then, a certain value from [1, 1.5, 2] is randomly generated for each demand point as the weight of the delivery package, and the total weight of the package delivery is less than or equal to 6 (the maximum payload of the drone), and the package delivery order is set to 0-1-2-3-3-4-0. The detailed experimental data is shown in Table 1 below.

Table 1. Experimental data

Demand point number	coordinate	map code	package weight
0	(31,5)	531	0
1	(8,33)	3308	1
2	(24,69)	6924	1.5
3	(82,60)	6082	1.5
4	(32,62)	6232	2

Note: The conversion formula between the demand point coordinates and map code (C) is:  $C = y_i * 100 + x_i$ , where  $(x_i, y_i)$  is the demand point coordinates and 100 is the total number of map rows (map width distance/grid granularity).

In this paper, the self-weight of UAV is set at 12kg and the battery weight is 2kg. The parameter values of the algorithm

are as follows: population size  $Z=1000$ , iteration number  $Gen=200$ , crossover probability  $p_c=0.8$ , mutation probability  $p_m=0.3$ . Other parameter Settings refer to relevant literature [5][8], and the specific values are shown in Table 2 below.

Table 2. Experimental parameter Settings

parameter	Numerical value
Maximum payload of UAV $Q_{max}/kg$	6
Flight speed $v_{ij}/(km/h)$	30
Battery's largest energy $E_{max}/(kW \cdot h)$	0.25
electronic components consumption $p/w$	100
Lift to drag ratio $\gamma$	3
power transfer efficiency for motor and propeller $\mu$	0.5
Risk cost weight coefficient $\omega_1$	0.5
Energy cost weight coefficient $\omega_2$	0.5
Risk penalty coefficient $K$	2
Grid granularity size $U/m$	10

## 4.2. Analysis of experimental results

This article uses Python 3.7 software programming, and the

path planning results obtained from simulation experiments are shown in Table 3. The path planning effect diagram is shown in Figure 4.

**Table 3.** Genetic Algorithm Path Planning Results

Road section number	Number of path points	Road length	Energy cost	Risk cost	Comprehensive cost
<b>[531] - [3308]</b>	33	493	0.0194	0.0366	0.028
<b>[3308] - [6924]</b>	37	466	0.0175	0.0345	0.026
<b>[6924] - [6082]</b>	59	683	0.0238	0.0582	0.041
<b>[6082] - [6232]</b>	29	399	0.0128	0.0852	0.049
<b>[6232] - [531]</b>	31	453	0.0129	0.0861	0.0495

According to Table 3, the total package weight for the drone path planning in the urban area is 6kg, with a total of 189 path points and a total flight path length of 2494m. The drone battery energy consumption is 0.0864kW · h, the flight risk cost is 0.3006, and the comprehensive cost is 0.1935 (comprehensive cost=0.5 × Battery energy cost+0.5 × Flight

risk cost), meeting maximum load and battery energy limitations. As shown in Figure 4, the path planning of this experiment effectively avoids all obstacles in the flight environment, and the path length is short, achieving a good balance between flight distance, energy consumption, and safety costs.

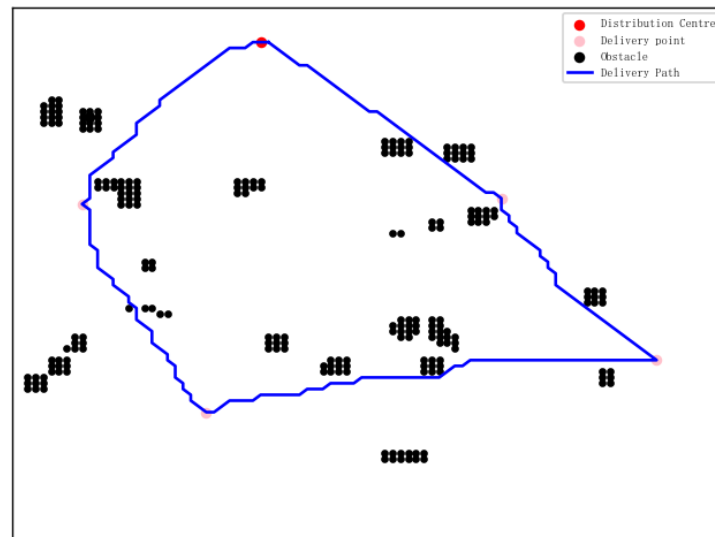


**Figure 4.** Path Planning Renderings

Due to the fact that the payload of drones is also an important factor affecting their flight energy consumption, especially when a single drone serves multiple delivery points, as the delivery task is completed, The load of a drone decreases (the load when the drone starts departure is X, assuming the package weight at the first delivery point is a, the load of the drone becomes X-a when the drone completes the first delivery task and starts the second delivery task, The weight of the following demand points and so on). Based on

this, this article adopts the energy consumption segmentation method to calculate the battery energy consumption generated by the drone during the delivery process. That is, when the drone completes the previous delivery task and proceeds to the next delivery task, Update the weight of the drone before calculating battery energy consumption. Among them, the calculated weight of energy consumption is the drone's self weight+load, and the comparison of experimental results is shown in Table 4:

**Table 4.** Comparison of segmented energy consumption calculation results

Road section number	No energy consumption segmentation		Energy consumption segmentation		Decline rate
	calculation weight	Battery energy consumption	calculation weight	Battery energy consumption	
<b>[531] - [3308]</b>	20	0.0194	20	0.0194	--
<b>[3308] - [6924]</b>	20	0.0183	19	0.0175	4.6%
<b>[6924] - [6082]</b>	20	0.0269	17.5	0.0238	11.4%
<b>[6082] - [6232]</b>	20	0.0157	16	0.0128	18.3%
<b>[6232] - [531]</b>	20	0.0178	14	0.0129	27.5%

From Table 4, it can be seen that under the same delivery path, considering the energy consumption segmentation method, the drone battery energy consumption decreases by 4.6% -27.5%. Meanwhile, the decrease rate of drone battery energy consumption increases with the completion of each delivery task. This is because in the mode of not considering segmented energy consumption, the weight carried by the drone remains unchanged during the calculation process. However, in the actual delivery process, the weight of goods

carried by a single drone when serving multiple delivery points decreases, especially when the drone no longer carries any goods by the final return journey, and its battery energy consumption will be smaller.

In order to remove too many zigzag 'z' paths, after the planning of the path is completed, the Freudian algorithm is used for path smoothing to remove adjacent collinear points and excess turning points. The optimization results are shown in Figure 5:

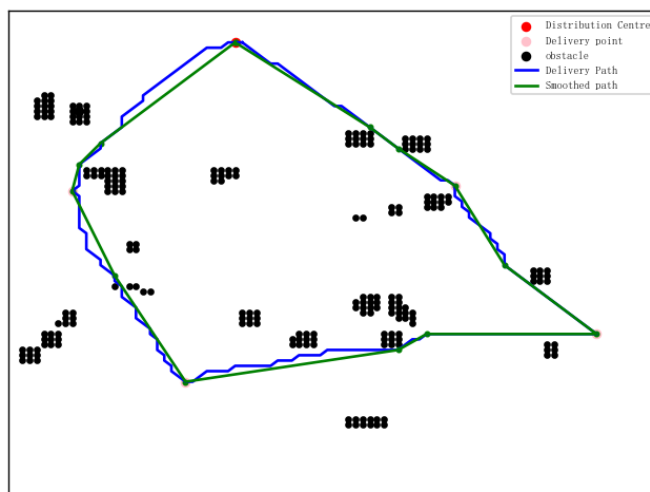


Figure 5. P Path map after path smoothing processing

From Figure 5, it can be seen that using the Freudian algorithm for path smoothing can remove redundant path points while ensuring the invariance of critical path points and safe obstacle avoidance, effectively reducing the zigzag 'z' path, which is more in line with the flying habits of unmanned aerial vehicles.

## 5. Conclusion

This article considers the logistics path planning of unmanned aerial vehicles in urban low altitude environments, with the goal of shortening flight paths, reducing energy consumption, and improving flight safety. A mathematical model is established. Firstly, use the grid method to complete urban environmental modeling, and then genetic algorithm is used for problem solving. The experimental results show that the model and algorithm proposed in this paper can effectively balance path length, battery energy consumption, and safety costs in unmanned aerial vehicle path planning. At the same time, it was also verified that using the energy consumption segmentation method to calculate the battery energy consumption of unmanned aerial vehicles is more accurate and practical.

## References

- [1] Y. Fan, K. Shen, D.Wang, et al. Optimal path planning for energy consumption in unmanned aerial vehicle mountain operations based on simulated annealing algorithm [J]. *Journal of Agricultural Machinery*, 2020,51 (10): 34-41.
- [2] H. Zhang, H. Li, H. Liu, et al. Urban Regional Logistics Drone Path Planning [J]. *Transportation System Engineering and Information*, 2020,20 (06): 22-29.
- [3] Y. Peng, Y. Li. Optimization of collaborative delivery routes for trucks and drones considering the impact of the epidemic [J]. *Journal of China Highway Engineering*, 2020,33 (11): 73-82.
- [4] W. Liu, W. Li, Q. Zhou, et al. Optimization Model and Algorithm for the Delivery Path of "Drone Vehicle" [J]. *Transportation System Engineering and Information*, 2021,21 (06): 176-186.
- [5] X. Ren, T. Wu. Logistics UAV Scheduling Model Considering Energy Consumption Segmentation [J]. *Computer Engineering and Applications*, 2022,58 (21): 301-308.
- [6] S. Huang, J. Tian, L. Qiao, et al. Path Planning for Unmanned Aerial Vehicles Based on Improved Genetic Algorithm [J]. *Computer Applications*, 2021,41 (02): 390-397.
- [7] Z. Zheng, S. Yang, Y. Zheng, et al. Multi rotor UAV obstacle avoidance path planning algorithm [J]. *Journal of agricultural engineering*, 2020,36 (23): 59-69.
- [8] Q. Zhang, W. Xu, H. Zhang, et al. Path planning for complex low altitude logistics unmanned aerial vehicles [J]. *Beijing University of Aeronautics and Astronautics Journal*, 2020,46 (07): 1275-1286.
- [9] J. Yang, H. Liu, X. Yang, et al. Path Planning for Mobile Robots Based on Genetic Algorithm [J]. *Mechanical and Electrical Engineering Technology*, 2020,49 (12): 97-98+117.
- [10] Z. Kewang and D. Tenghuan, "Research on Obstacle Avoidance Control Method of Multi-UAV Based on Model Predictive Control," 2021 International Conference on Electronics, Circuits and Information Engineering (ECIE), Zhengzhou, China, 2021, pp. 357-362.
- [11] D'Andrea,Raffaello. Guest editorial can drones deliver?[J] *IEEE Transactions on Automation Science &Engineering* 2014, 11(3):647-648.